



Research Article

Molecular Cloning, Expression, and Sub-Cellular Localization of MGLL in NSCLC Cell Lines

 Youssra Boustany,^{1,2}  Abdelilah Laraqui,^{1,3}  Mohammed Oukabli,⁴  Yassine Sekhsokh,¹  Bouchra Belkadi,²
 Steven Gray⁵

¹Research and Biosafety Laboratory, Mohamed V Military Teaching Hospital, Faculty of Medicine and Pharmacy, Mohammed V University in Rabat, Morocco

²Microbiology and Molecular Biology Team, Faculty of Sciences, Mohammed V University in Rabat, Morocco

³Sequencing Unit, Virology Laboratory, Virology Center of infectious and tropical diseases, Mohamed V Military Teaching Hospital, Faculty of Medicine and Pharmacy, Mohammed V University in Rabat, Morocco

⁴Anatomopathology Laboratory, Mohamed V Military Teaching Hospital, Faculty of Medicine and Pharmacy, Mohammed V University in Rabat, Morocco

⁵Thoracic Oncology Research Group, Laboratory Medicine and Molecular Pathology, Central Pathology Laboratory, St. James's Hospital, Dublin, Ireland

Abstract

Objectives: Monoglyceride lipase (MGLL), as a prominent metabolic hub, is known to be actively involved in the development of the lipogenic phenotype, which promotes *de novo* lipid biosynthesis, allowing cancer cells to maintain their growth advantage, continuous proliferation, and metastasis. In this study, we aim to investigate mRNA MGLL expression levels and its sub-cellular localization in non-small cell lung cancer (NSCLC) cell lines, as well as examine the effect of two chemotherapy/targeted therapy agents, cisplatin and crizotinib, on the expression levels of MGLL.

Methods: pcDNA3.1(-)-MGLL and pEGFPN1-MGLL constructs were sub-cloned into *E.coli* DH5a and transfected into NSCLC cell lines for MGLL expression evaluation and sub-cellular localization, using polymerase chain reaction (PCR) and quantitative PCR (qPCR) and fluorescence microscopy, respectively. Parent and cisplatin/crizotinib-resistant cell lines were grown and maintained in adequate media for subsequent MGLL expression analysis.

Results: PCR and qPCR results revealed that MGLL was successfully transfected into the H1299 cells and efficiently expressed. Fluorescence microscopy of the pEGFPN1-MGLL transfected cells revealed a cytosolic expression of MGLL. As per the analysis on the effect of cisplatin and crizotinib on MGLL expression, a notable downregulation of MGLL expression was noted in the resistant cell lines.

Conclusion: These results provide groundwork for further research on molecules modulating MGLL expression, which may be deemed helpful to provide therapy options targeting MGLL in NSCLC treatment.

Keywords: Lung cancer, MGLL expression, pcDNA3.1, cisplatin

Cite This Article: Boustany Y, Laraqui A, Oukabli M, Sekhsokh Y, Belkadi B, Gray S. Molecular Cloning, Expression, and Sub-Cellular Localization of MGLL in NSCLC Cell Lines. *EJMO* 2022;6(4):330–338.

Lung cancer is the most common cause of cancer-related deaths worldwide and the second leading malignancy in terms of incidence.^[1] Of the two main lung cancer types,

non-small cell lung cancer (NSCLC) represents 80%–85% and includes three main histologic subtypes, namely, lung adenocarcinoma, squamous cell carcinoma (SCC), and

Address for correspondence: Youssra Boustany, PhD. Research and Biosafety Laboratory, Mohamed V Military Teaching Hospital, Faculty of Medicine and Pharmacy, Mohammed V University in Rabat, Morocco; Microbiology and Molecular Biology Team, Faculty of Sciences, Mohammed V University in Rabat, Morocco

Phone: +212 660099025 **E-mail:** youssra.boustany@um5s.net.ma

Submitted Date: July 15, 2022 **Accepted Date:** October 26, 2022 **Available Online Date:** December 30, 2022

©Copyright 2022 by Eurasian Journal of Medicine and Oncology - Available online at www.ejmo.org

OPEN ACCESS This work is licensed under a Creative Commons Attribution-NonCommercial 4.0 International License.



large cell carcinoma (LCC), with lung adenocarcinoma being the most prevalent (40%).^[2] Despite significant progress in lung cancer management, the 5-year overall survival is only at 19%.^[3] This is largely attributed to late diagnosis and the lack of potent and selective therapeutic agents on one hand and accurate targets for precision medicine drugs on the other hand;^[4] hence, there is an imperious necessity to support promising therapeutic targets for cancer treatment.

The role of lipid metabolism in cancer has gained increasing attention in recent years. Emerging evidence have linked dysregulated lipid metabolism to promoting oncogenesis and cancer progression.^[5] During carcinogenesis, a progressive metabolic shift is often observed, favoring *de novo* lipid biosynthesis, characterized by a heightened fatty acid synthesis. This provides bioactive lipids acting as signaling molecules and components for new membranes, thus allowing cancer cells to maintain their growth advantage, continuous proliferation, metastasis, and invasion.^[6, 7] Aberrations in the expression of genes involved in fatty acid synthesis or fatty acid oxidation have been found to correlate with malignant phenotypes, including metastasis and drug resistance.^[8]

Monoacylglycerol lipase (MGLL) is a 33 kDa serine hydrolase enzyme in which its gene locus is on human chromosome 3q21.3.^[9] MGLL catalyzes the hydrolysis of triacylglycerol (TAG) to produce fatty acids (FFA) and modulates the endocannabinoid and eicosanoid lipid signaling network, as it catalyzes the hydrolysis of 2-arachidonoylglycerol (2-AG), which is an endogenous ligand of the cannabinoid receptors 1 and 2 (CB1 and CB2, respectively), into arachidonic acid and glycerol.^[10] Adversely, MGLL has been found to be highly expressed in various cancers and is identified to promote tumorigenesis and cancer metastasis through its modulation of the fatty acid network.^[11, 12] In NSCLC, MGLL expression was shown to be downregulated, but the underlying processes by which MGLL promotes tumorigenesis and metastasis are yet to be elucidated.^[13]

In this study, we explored different facets of MGLL expression in NSCLC by investigating mRNA MGLL expression levels and its sub-cellular localization in NSCLC cell lines, as well as the effect of the two most commonly used chemotherapy/targeted therapy agents, cisplatin and crizotinib, on the expression levels of MGLL.

Methods

Cell Lines and Cell Culture

The NSCLC cell lines used in this study are A549 and the cisplatin-resistant A549, which are hypotriploid alveolar

basal epithelial cells; the H1299 and the cisplatin-resistant H1299, a cell line derived from the lymph node; the H3122 and the crizotinib-resistant H3122, a cell line characterized with an ALK translocation; the H2030 cell line, a NSCLC p53 and RAS mutated cell line; and the H1975 cell line, a NSCLC EGFR, PIK3CA, and p53 mutated cell line. The A549 and the cisplatin-resistant A549 were cultured in Nutrient Mixture F-12 Ham medium containing 0.5 % fetal bovine serum (FBS, Gibco, CA), 0.1% PSA antibiotics (Penicillin-Streptomycin-Amphotericin Solution), and 2.0 mM-glutamine, while the other used cell lines were cultured in RPMI-1640 medium (CORNING, 10-040-CVR) supplemented with 0.5 % fetal bovine serum (FBS, Gibco, CA), 0.1% PSA antibiotics (Penicillin-Streptomycin-Amphotericin Solution), and 2.0 mM-glutamine, all at 37°C in a humidified atmosphere containing 5% CO₂.

Bacterial Strain and Plasmids

E. coli DH5a competent cells were used in the sub-cloning of MGLL. They are known to have a high transformation efficiency, emanating from their *recA1* and *endA1* characterizing mutations. They are also characterized by the *lacZ*ΔM15 mutation that enables blue-white screening.

pcDNA3.1(-) expression vector and pEGFP-N1 fusion vector were used in MGLL overexpression and cellular sub-localization tests, respectively.

Gene Amplification

The full-length MGLL open reading frame was amplified, from a cDNA library, using a designed primer set (Forward: CGTTTCGTCAGGGATGTGTT Reverse: CCAGAGGCGAAATGAGTACCA). A PCR reaction was carried out in a final reaction of 21 μl in 0.5 ml micro-tubes containing 1 μg of template DNA, 10 μl of Dream Taq Green Master Mix (Thermo Scientific), 6 μl of molecular grade water, and 2 μM of each primer. One μl of molecular grade water, instead of template DNA, was used as negative control. PCR reaction was performed with initial denaturation at 95 °C for 10 min, followed by 35 thermal cycles at 95 °C for 1 min, 58 °C for 2 min, and 72 °C for 2 min. Final extension was carried out at 72 °C for 10 min. Amplified PCR products were analyzed by electrophoresis in 0.8% agarose gel. Subsequently, the PCR products were band isolated and purified using the Promega Wizard kit and then measured using the NanoDrop spectrophotometer (LabTech International, Ringmer, UK).

Cloning of MGLL into pcDNA3.1(-) and pEGFP-N1

Based on restriction enzyme mapping of MGLL and the multiple cloning sites present in pcDNA3.1(-) and pEGFP-N1 vectors, EcoR V/BamH I and Xho I/BamH I were chosen as the insertion sites for MGLL cloning in pcDNA3.1(-)

and pEGFP-N1, respectively. Two primer sets were designed, and restriction enzymes sites were inserted, containing a Kozak consensus sequence and in-frame translation stop signals. When cloning into the pEGFPN1 fusion vector, MGLL must be in the same reading frame as the downstream EGFP gene sequence to ensure co-expression of the fusion protein.

The purified MGLL fragments and the pcDNA3.1(-) expression plasmid were double digested overnight at 37°C with EcoRV/BamH I and then purified with the Promega Wizard kit. The purified MGLL fragments and the pEGFPN I vector were also digested overnight at 37°C with Xho I/BamH I and then purified with the Promega Wizard kit.

The enzyme reaction contained 2 µl of target gene fragment (or vectors), 2 µl of buffer 3, 2 µl of BSA 10x buffer, 1 µl of restriction enzyme, and up to 20 µl of molecular grade water.

To generate the recombinant plasmids, pcDNA3.1(-)-MGLL and pEGFPN I-MGLL, two separate ligation reactions were realized, in either a 1:1 or 3:1 (insert/vector) ratio. The ligation reaction contained 2 µl of 10x T4 DNA ligase buffer, 1 µl T4 DNA ligase, the appropriate volume of insert and vector (for either the 1:1 or 3:1 (insert/vector) ratio reaction), and molecular grade water up to 20 µl. The reactants were well mixed and incubated at 16°C overnight.

Sub-Cloning of MGLL Into *E. coli* DH5a

The ligated products, pcDNA3.1(-)-MGLL and pEGFPN I-MGLL, were transformed into competent *E. coli* DH5a, with the specific steps as follows: incubation on ice (-6°C) for 30 min, heat stress at 42°C for 45 s, and then cold stress (-6°C) for 1 min. The pcDNA3.1(-)-MGLL transformants were selected on LB-ampicillin agar plates, while the pEGFPN I-MGLL transformants were selected on LB-Kanamycin agar plates. Transformed colonies were isolated, and a random analysis of ten clones was then conducted using PCR. Positive clones were shaken in a thermostatic culture cradle overnight at 37°C. Plasmids were extracted from the overnight-grown bacteria using PureYield™ Plasmid Midiprep System kit (Promega), and DNA concentration and quality were determined using the NanoDrop spectrophotometer (LabTech International, Ringmer, UK). To test for insert orientation, the pcDNA3.1(-)-MGLL construct was digested with EcoRV/BamH I and SalI/BamH I, whereas the pEGFPN I-MGLL construct was digested with Pst I/BamH I, Sal I/BamH I, Xho I/Pst I, and Xho I/Sal I and then evaluated by agarose gel electrophoresis.

Transfection of pcDNA3.1(-)-MGLL and pEGFPN I-MGLL into NSCLC Cell Lines

The H1299 cell lines were used to study MGLL expression,

and A549, H3122, H2030, H1975, and H1299 were used to identify MGLL expression and sub-cellular localization. Both pcDNA3.1(-)-MGLL and pEGFPN I-MGLL constructs were transfected into the cells using FuGENE. Twenty-four hours before the transfection, and as the cells reached the logarithmic growth phase, 1×10^5 cells were seeded in a 12-well plate. The cells were maintained in triplicates and divided into four distinct groups: untreated cells, cells with transfection agent (FuGENE), empty vector control, and vector-MGLL construct. To transfect the vector-MGLL construct into the cells, 2000 ng of DNA (MGLL and vectors) was diluted into 100 µl of RPMI, while 3 µl of FuGENE was diluted in a final volume of 100 µl of RPMI. Vector-MGLL constructs and FuGENE were mixed and allowed to react for 15 min at room temperature. Subsequently, the FuGENE:DNA complex was added to cells in a drop-wise manner. The wells were swirled to ensure distribution over the entire plate surface. Then, 24 to 72 hours after the transfection, the cells were harvested, and total RNA was isolated for MGLL expression evaluation. As for the pEGFPN I-MGLL transfected cell lines, 24–72 hours after the transfection, cells were visualized under EVOS FL Auto 2 Cell Imaging System (Thermo Fisher Scientific).

RNA Extraction and cDNA Synthesis

Total RNA was extracted, from both the cultured parent and cisplatin/crizotinib-resistant cell lines and from the H1299 transfected cell line for MGLL expression evaluation, using TRI Reagent® and following the manufacturer's instructions. The quantity and quality of RNA were determined by NanoDrop spectrophotometer (LabTech International, Ringmer, UK), and RNA was diluted and stored for subsequent tests.

First-strand cDNA was synthesized from the isolated RNA starting with genomic DNA denaturation using DNase in a reaction buffer. The mix was incubated for 15 min at room temperature. After adding the stop solution, the mix was incubated for 10 min at 70°C. Ready Script cDNA Master Mix® and molecular grade water were added to the mix to synthesize cDNA.

During first-strand cDNA synthesis, appropriate negative and positive controls were included in the analysis to ensure that the presence or absence of the expected product does not result from contamination or lack of template.

PCR Analysis

Polymerase chain reaction (PCR) was used to assess MGLL expression in both the cultured parent and cisplatin/crizotinib-resistant cell lines and in the H1299 transfected cell line. The newly synthesized cDNA was amplified using a designed primer set (Forward: CGTTTCGTCAGGGATGT-

GTT Reverse: CCAGAGGCGAAATGAGTACCA). A PCR reaction was carried out in a final reaction of 21 μ l in 0.5 ml micro-tubes containing 1 μ g of template DNA, 10 μ l of Dream Taq Green Master Mix (Thermo Scientific), 6 μ l of molecular grade water, and 2 μ M of each primer. Moreover, 1 μ l of molecular grade water, instead of template DNA, was used as negative control. PCR reaction was performed with initial denaturation at 95°C for 10 min, followed by 35 thermal cycles at 95°C for 1 min, 58°C for 2 min, and 72°C for 2 min. Final extension was carried out at 72°C for 10 min. 18S rRNA served as a housekeeping gene and was amplified in a PCR mixture made as mentioned earlier. Equal amounts of MGLL and 18S PCR products were electrophorized on a 0.8% agarose gel and visualized under UV light by ethidium bromide staining.

Real-Time PCR Analysis

Real-time quantitative polymerase chain reaction was performed in duplicates to analyze MGLL mRNA expression in both the cultured parent and cisplatin/crizotinib-resistant cell lines and in the H1299 transfected cell line. 18S rRNA served as a housekeeping gene. We used the StepOnePlus Real-Time PCR System (Applied Biosystems). The $\Delta\Delta$ Ct method and StepOne software (Applied Biosystems) were used to calculate expression levels. Each RT product was run on a 96-well optical plate in a total volume of 21 μ l/well including 1 μ l RT product, 2 μ l of each primer (Forward: CGTTTTTCGTCAGGGATGTGTT Reverse: CCAGAGGCGAAATGAGTACCA), 6 μ l of molecular grade water, and 10 μ l SYBR qPCR Mix, using the following profile: 95°C for 10 min, and 40 cycles of 95°C for 15 sec and 58°C for 45 sec. A dissociation step was performed following the qPCR amplification for melting curve analysis.

Results

MGLL Expression in H1299 NSCLC Cells

MGLL full-length fragment was band isolated and purified after PCR amplification. The PCR fragment and the pcDNA 3.1(-) expression plasmid were then digested overnight at 37°C with EcoR V and BamH I and then purified with the Promega Wizard kit. Subsequently, MGLL was ligated into pcDNA 3.1 (-) in either a 1:1 or 3:1 (insert/vector) ratio. pcDNA 3.1 (-)-MGLL construct was transformed into chemically competent DH5a *E. coli* that were then plated onto appropriate selective antibiotic (ampicillin). Ten colonies of each were isolated as above and assessed for the presence of the insert using PCR. A medium-scale midi-prep of the PCR-positive clones was carried out, isolating the pcDNA 3.1 (-)-MGLL construct, using the Promega PureYield Plasmid Midiprep System. The isolated recombinant plasmid

was digested with EcoR V/BamH I and Sal I/BamH I and ran on agarose gel electrophoresis, producing the expected fragments (Fig. 1). The pcDNA3.1(-)-MGLL construct was then transfected into H1299 cells as described previously. The cells were maintained in biological triplicates and divided into four distinct groups: untreated cells, cells with transfection agent, empty vector control, and pcDNA3.1(-)-MGLL construct. Then, 24–72 hours after the transfection, the cells were harvested, and total RNA was isolated for cDNA synthesis.

An initial MGLL expression analysis was carried out using PCR. As shown in Figure 2, MGLL expression was clearly higher in the pcDNA 3.1 (-)-MGLL group as compared to the untreated cells group, the cells with transfection agent group, and the empty vector control group, indicating that MGLL was successfully transfected into the H1299 cells and efficiently expressed. This was the case for the three replicates. The 18S rRNA expression levels, however, were stable across the four groups and the three repeats, as expected.

To further validate these results, a qPCR analysis of MGLL expression was carried out. The amplification specificity was validated by melting curve analysis generated at the end of the qPCR reaction. MGLL, as well as the 18S reference gene, presented a single peak in the melting curve, which indicated the absence of primer-dimer formation

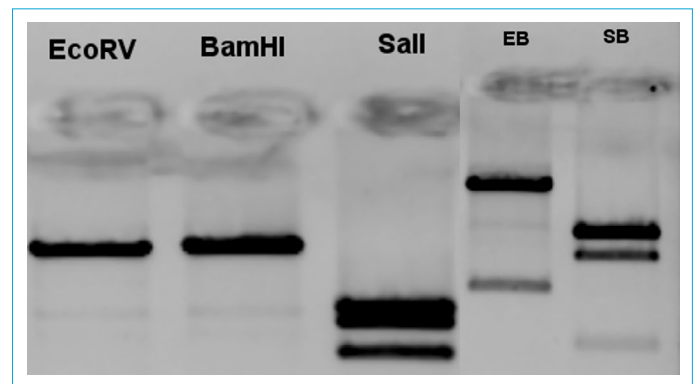


Figure 1. Evaluation of MGLL insertion orientation in pcDNA 3.1 (-).

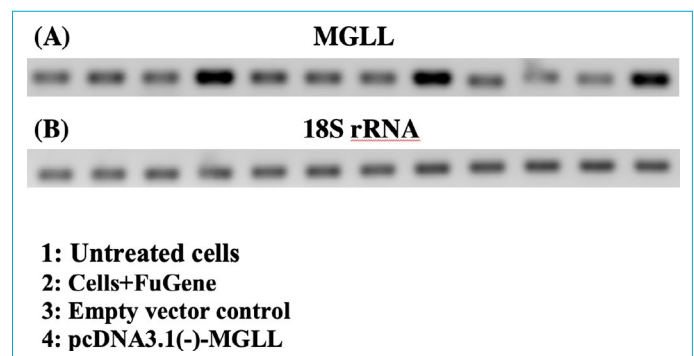


Figure 2. MGLL expression evaluation in the transfected H1299 cell line.

during the reaction and specificity of the amplification. Amplification efficiency was then checked by monitoring the slope of amplification curves generated during real-time amplification, while specificity was confirmed by analyzing the uniqueness of the PCR product by melting curve peak analysis. Gene expression was evaluated comparing Ct values between pcDNA 3.1(-)-MGLL group and untreated cells, cells with transfection agent, and empty vector control groups, using the $\Delta\Delta CT$ method. Notably, pcDNA3.1(-)-MGLL transfected cells showed a clear increase of MGLL expression in comparison to the other three groups (Fig. 3).

MGLL Expression and Sub-Cellular Localization

MGLL full-length fragment was generated via PCR. After electrophoresis on agarose gel, the fragment was isolated and purified. Subsequently, the PCR fragment as well as the pEGFPN 1 fusion vector were separately digested overnight at 37°C with Xho I/BamH I and then purified with the Promega Wizard kit. Thereafter, MGLL was ligated into pEGFPN 1 in either a 1:1 or 3:1 (insert/vector) ratio. pEGFPN 1-MGLL construct was then transformed into chemically competent DH5a *E.coli* that were then plated onto appropriate selective antibiotic (kanamycin). Blue-white screening allowed for the selection of recombinant colonies. These colony transformation was validated using PCR. Electrophoresis showed which colonies express the insert. These were grown overnight in a liquid media in 37°C. A medium-scale midi-prep of the PCR-positive clones was carried out, isolating the pEGFPN 1-MGLL construct, using the Promega PureYield Plasmid Midiprep System. The isolated recombinant plasmid was digested with the following to test for insert orientation: (a) Pst I / BamH I, expected fragment 133 bases; (b) Sal I / BamH I, expected fragment 340 bases (c) Xho I / Pst I, expected fragment 127 bases; and (d) Xho I / Sal I, expected fragment 601 bases (Fig. 4). The

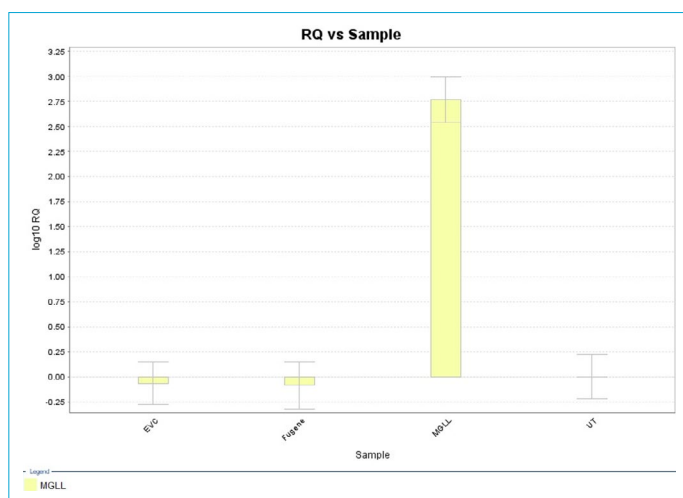


Figure 3. MGLL expression in the transfected H1299 cell line.

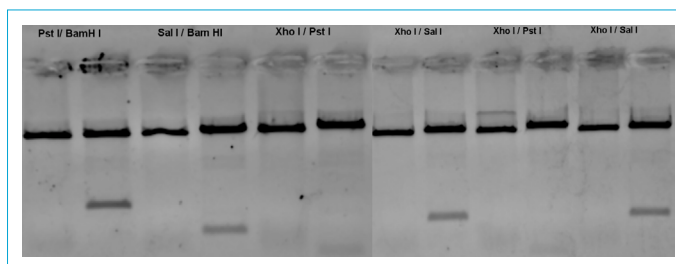


Figure 4. Evaluation of MGLL insertion orientation in pEGFPN 1.

pEGFPN 1-MGLL construct was then transfected into the A549, H1299, H2030, H3122, and H1975 cells as described previously. The cells were divided into four distinct groups: untreated cells, cells with transfection agent, empty vector control, and pEGFPN 1-MGLL construct. Then, 48 hours after the transfection, the cells were visualized using EVOS FL Auto 2 Cell Imaging System (Thermo Fisher Scientific).

The expression of the EGFP reporter gene was clearly observed using fluorescence microscopy in the pEGFPN1-MGLL and the pEGFPN1 group, but not in the control groups. The results revealed that in the pEGFPN1-MGLL and the pEGFPN1 group, large numbers of A549, H1299, H1975, H2030, and H3122 cells expressed GFP, suggesting that pEGFPN1-MGLL construct and pEGFPN1 empty fusion vector have been effectively transfected into the cells (Fig. 5). It was expected that the pEGFPN1 group would express a more intense fluorescence signal than the pEGFPN1-MGLL group, since the empty pEGFPN1 fusion vector was smaller and had a higher transfection efficiency. It was found that in the pEGFPN1-MGLL group, the fluorescence emanated from the cytosol of the transfected cell lines, suggesting a cytosolic sub-cellular localization of MGLL expression.

MGLL Expression in Parent vs Cisplatin/Crizotinib-Resistant A549, H1299, and H3122 Cells

To assess the discrepancies in MGLL expression between parent and cisplatin/crizotinib-resistant cell lines, the A549

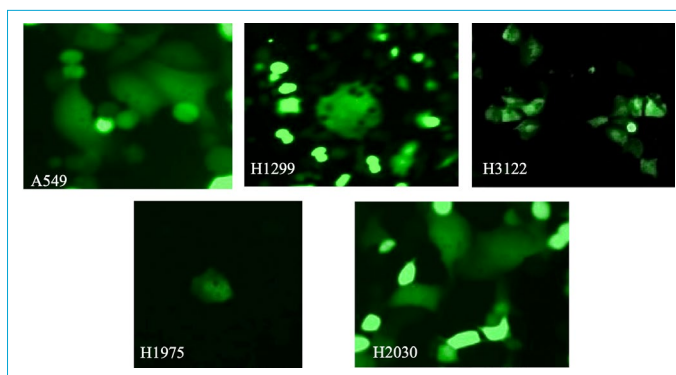


Figure 5. Sub-cellular localization of MGLL expression in the transfected cell lines.

and the cisplatin-resistant A549, the H1299 and the cisplatin-resistant H1299, and the H3122 and the crizotinib-resistant H3122 cell lines were grown in triplicates. MGLL expression was therefore analyzed in 18 distinct cell line measurements, each measured in duplicates across the biological triplicates.

The cells were grown in adequate conditions as described previously. As the cells reached the logarithmic growth phase, they were harvested, and RNA was isolated for cDNA synthesis. Preliminarily, MGLL was assessed across the parent and cisplatin/crizotinib-resistant cell lines using PCR. As illustrated in Figure 6, MGLL appears to be downregulated in cisplatin/crizotinib-resistant A549, H1299, and H3122 cell lines, as MGLL expression was notably lower in the resistant cell lines relative to the parent cell lines across the board and in the three repeats. As expected, 18S rRNA expression was shown to be stable in all the triplicated cell lines.

MGLL expression in parent vs cisplatin/crizotinib-resistant A549 and H3122 cell lines was further validated using qPCR. The analysis of the melting curve generated was indicative of the quality of the absence of primer-dimer formation during the reaction and specificity of the amplification. The analysis showed a clear downregulated expression of MGLL in cisplatin/crizotinib-resistant cell lines relative to parental cell lines (Fig. 7).

Discussion

The growing interest that lipid metabolism has acquired in recent years has shed light on the implication of the altered expression of genes involved in fatty acid synthesis or fatty acid oxidation in malignant phenotypes, including metastasis and drug resistance.^[14] MGLL, as a prominent metabolic hub, is known to be actively involved in the lipogenic phenotype, favoring *de novo* lipid biosynthesis. In cancer, lipogenesis is characterized by a heightened fatty acid synthesis, which has been determined to provide bioactive lipids acting as signaling molecules and building blocks for new membranes, allowing cancer cells to maintain their growth advantage, continuous proliferation, metastasis, and invasion.^[15,16]

In this study, we explored different facets of MGLL expression in NSCLC by investigating mRNA MGLL expression levels and its sub-cellular localization in NSCLC cell lines, as well as the effect of the two most commonly used chemotherapy/targeted therapy agents, cisplatin and crizotinib, on the expression levels of MGLL. The transfection of H1299 cells with the pcDNA 3.1(-)-MGLL construct showed that MGLL was successfully transfected into the H1299 cells and efficiently expressed. Furthermore, fluoroscopic mi-

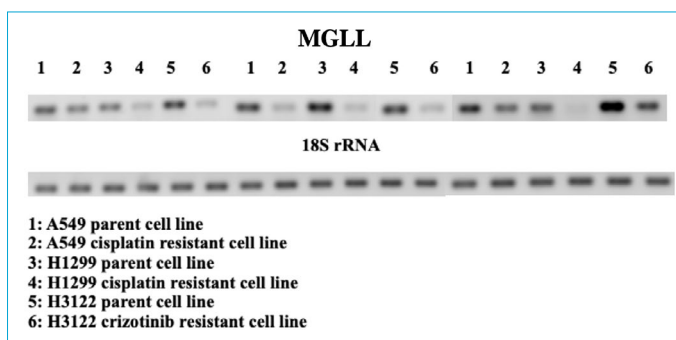


Figure 6. MGLL expression analysis in parent vs cisplatin/crizotinib resistant A549, H1299, and H3122 cell lines.

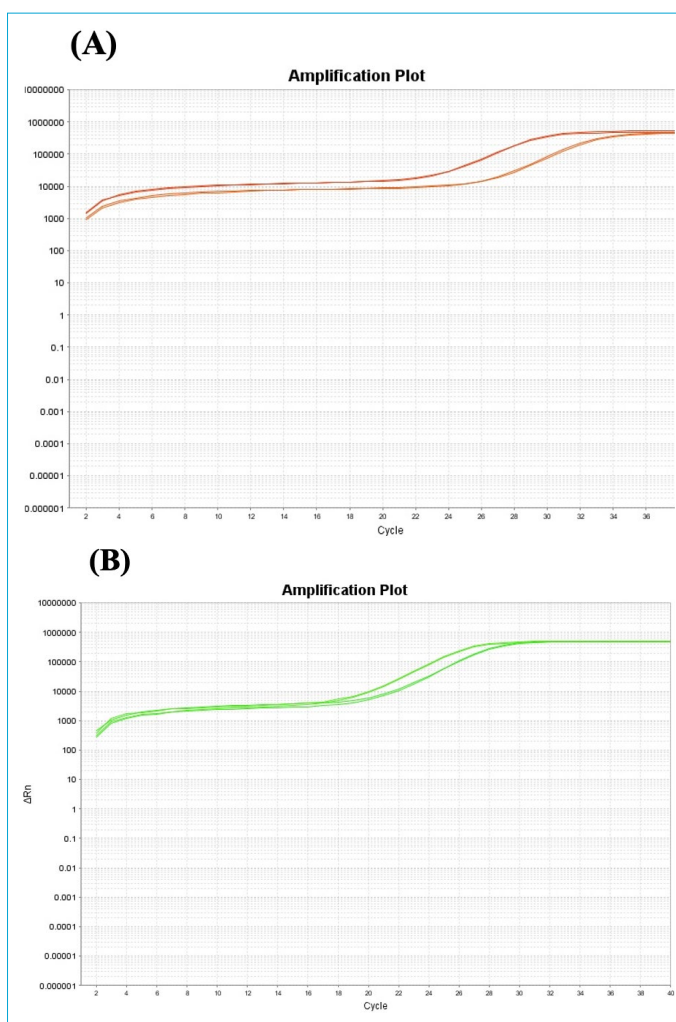


Figure 7. MGLL expression analysis in parent vs resistant cisplatin/crizotinib cell lines. (a) MGLL expression analysis in parent vs cisplatin resistant A549 cell line. (b) MGLL expression analysis in parent vs crizotinib resistant H3122 cell line.

croscopy visualization of pEGFPN 1-MGLL-transfected cell lines revealed that the pEGFPN 1-MGLL group expressed a fluorescence signal emanating from the cytosol of the cells, which indicates a cytosolic sub-cellular localization of MGLL expression.

Previous studies have reported that MGLL is expressed in various tumors including lung adenocarcinoma,^[15] hepatocellular carcinoma,^[17] colorectal cancer,^[18] endometrial cancer,^[19] gastrointestinal stromal cancer,^[20] and prostate cancer.^[21] Additionally, it was shown that MGLL mRNA expression was downregulated in cancers of the colon (59.4%), rectum (50%), stomach (50%), breast (61%), and ovary (50%).^[13] In lung cancer, it has been reported that MGLL was downregulated in lung cancer tissue, promoting tumor development in several organs including the lungs, lymphoid tissues, liver, and soft tissues in mice. MGLL deficiency was found to particularly favor the development of adenocarcinomas in animal models; however, the underlying processes are yet to be elucidated.^[13] Conversely, in a study by Zhang et al., it was found that MGLL was upregulated in LUAD tissues, and MGLL expression levels were significantly correlated with overall survival. They also found that MGLL knockdown inhibits cancer cell proliferation both *in vitro* and *in vivo*.^[11]

MGLL implication in a wide variety of tumors can stem from its association with tumor-related signaling pathways, the most common of which is the PI3K-AKT signaling pathway. This pathway is known to be involved in various cellular processes, including metabolism, growth, proliferation, survival, transcription, and protein synthesis.^[23, 25] It has been shown that MGLL may structurally inhibit AKT phosphorylation, suggesting a potential negative regulatory effect of MGLL on the PI3K-AKT pathway. The MGLL-FFA pathway can regulate numerous lipid networks that involve a variety of potential tumorigenic signaling molecules, promoting tumor growth and cell migration.^[12] Moreover, MGLL is known to be involved in processes such as cytokine-cytokine receptor interaction, neuroactive ligand-receptor interaction, and retrograde endocannabinoid signaling.^[11] Also, it has been reported that MGLL is implicated in Kruppel-like factor 4 (KLF4) and NF- κ B signaling pathways.^[24]

In NSCLC, it was shown that aberrations in MGLL expression were associated with important molecular alterations. Liu et al. have shown that EGFR, one of the most prominent biomarkers in lung cancer, can be affected by MGLL expression in various ways. It has been reported that MGLL downregulation correlated with increased expression and phosphorylation of EGFR. Another way by which MGLL indirectly modulates EGFR expression is through negatively regulating both ERK and Akt signals, which, in turn, positively modulates EGFR expression. Furthermore, MGLL may regulate EGFR via a transcription-independent mechanism, since EGFR levels are also modulated by protein-protein interaction, endocytosis, and protein turnover/degradation. Furthermore, it has been also found that, *in vitro*, MGLL downregulated expression is linked to heightened COX-2

mRNA and protein levels.^[13] In keeping with MGLL's role in regulating modulators of inflammatory response in lung cancer, it has been found that the expression of pro-inflammatory cytokine TNF- α was also significantly elevated in MGLL-deficient lung tissues.^[13]

A previous study was able to determine the cellular localization of MGLL protein using immunofluorescent staining with an MGLL-specific antibody in HT29 colon cancer cells. They found that MGLL was mainly detected in the cytosol with a punctate expression pattern. In HCT116 colon cancer cells and NIH3T3 mouse fibroblasts, the same patterns were reported. As this punctate staining pattern is characteristic of the mitochondria, the endoplasmic reticulum (ER), and cytosolic lipid droplets, Sun et al. sought to determine which of these cellular organelles is home to the MGLL protein. The results indicate that MGLL is predominantly distributed to the core surface of the cytosolic lipid droplet and formed "MGLL crescents" around the cytosolic lipid droplet. Therefore, these findings indicate that MGLL is a cytosolic lipid droplet-associated protein.^[22]

Furthermore, our results have shown that two of the most commonly used chemotherapy/targeted therapy agents, cisplatin and crizotinib, had a remarkable effect on MGLL expression, as levels of MGLL mRNA expression were notably higher in A549, H1299, and H3122 parent cells than they were in cisplatin-resistant A549 and H1299 and crizotinib-resistant H3122 cells, evident of a clear downregulation of MGLL in cisplatin/crizotinib-resistant cell lines. These results are indicative of the effect that chemotherapy/targeted therapy agents have on MGLL expression to counter its tumorigenic role. In a previous study, we have found that MGLL expression in NSCLC can be affected by various chemotherapy agents: for example, paclitaxel and topotecan can elevate the expression level of MGLL, while cisplatin, oxaliplatin, and doxorubicin can reduce MGLL expression. Additionally, sunitinib, which is a tyrosine kinase inhibitor, was found to increase the expression of MGLL mRNA.

Inhibition of MGLL expression and function has been explored in many studies, as MGLL has a number of implications in many pathologies and disorders. In cancer, considerable efforts have been made to explore cannabinoid anticancer virtues since the discovery of Δ^9 -THC and other phytocannabinoids that have potential to reduce the rate of growth of lung tumor xenografts.^[25] In a study by Nithipatikom et al., it was found that the CB receptor agonist noladin ether reduced the *in vitro* invasiveness of androgen-independent human DU145 and PC-3 prostate cancer cells.^[26] In xenograft models of ovarian, melanoma, and colorectal cancers, JZL184 treatment and genetic knock-

down of MGLL have been found to reduce the tumor sizes.^[27] JZL184 was also found to decrease tumor growth and enhance sensitivity to chemotherapy, as Ma et al. demonstrated that tumor cell proliferation was reduced and apoptosis increased in response to MGLL inhibition and that the treatment with JZL184 and 5-fluorouracil induced greater cell apoptosis than 5-fluorouracil alone in colorectal cancer cell lines.^[28] In keeping with JZL184's ability to enhance sensitivity to chemotherapy, a study by Gong et al. reported that JZL184 can re-sensitize MG-63/R cells to cisplatin treatment. Additionally, the study indicates that MGLL inhibition suppresses the proliferation, clone formation, invasion, and migration of osteosarcoma cells *in vitro* by regulating EMT-related proteins.^[29] As such, there is a strong interest in the development of potent and accurate MGLL inhibitors for the treatment of cancers. This will simultaneously require gaining a better insight into the mechanisms and processes by which MGLL is implicated in malignant phenotypes, supporting MGLL as a therapeutic target for cancer treatment.

In summary, the generated pcDNA 3.1(-)-MGLL has been successfully constructed wherein it was found to demonstrate biological activity by expressing MGLL in the NSCLC H1299 cell line. Also, our study can potentially provide insight into MGLL expression and sub-cellular localization in NSCLC, as results from pEGFPN1-MGLL transfected with A549, H2030, H1975, H3122, and H1299 revealed a cytosolic localization of MGLL expression. Our results on down-regulated MGLL expression in cisplatin/crizotinib-resistant A549, H1299, and H3122 cell lines provide groundwork for further research on treatment options modulating MGLL expression, which may be helpful to provide effective and accurate therapy agents targeting MGLL in lung cancer treatment.

Disclosures

Ethics Committee Approval: The study was approved by the Local Ethics Committee.

Peer-review: Externally peer-reviewed.

Conflict of Interest: None declared.

Authorship Contributions: Concept – S.G.; Design – S.G.; Supervision – S.G.; Materials – S.G.; Data collection &/or processing – Y.B.; Analysis and/or interpretation – Y.B.; Literature search – Y.B.; Writing – Y.B.; Critical review – B.B., A.L., M.O., Y.S.

References

1. Bray F, Ferlay J, Soerjomataram I, Siegel RL, Torre LA, Jemal A. Global cancer statistics 2018: GLOBOCAN estimates of incidence and mortality worldwide for 36 cancers in 185 countries. *CA Cancer J Clin* 2018;68:394–424. [\[CrossRef\]](#)
2. Planchard D, Popat S, Kerr K, Novello S, Smit EF, Faivre-Finn C, et al; ESMO Guidelines Committee. Metastatic non-small cell lung cancer: ESMO Clinical Practice Guidelines for diagnosis, treatment and follow-up. *Ann Oncol* 2018;29:iv192–iv237.
3. Siegel RL, Miller KD, Jemal A. Cancer statistics, 2019. *CA Cancer J Clin* 2019;69:7–34. [\[CrossRef\]](#)
4. Xiao X, Shan H, Niu Y, Wang P, Li D, Zhang Y, et al. TMPRSS2 serves as a prognostic biomarker and correlated with immune infiltrates in breast invasive cancer and lung adenocarcinoma. *Front Mol Biosci* 2022;9:647826. [\[CrossRef\]](#)
5. Li CF, Chuang IC, Liu TT, Chen KC, Chen YY, Fang FM, et al. Transcriptomic reappraisal identifies MGLL overexpression as an unfavorable prognosticator in primary gastrointestinal stromal tumors. *Oncotarget* 2016;7:49986–97. [\[CrossRef\]](#)
6. Menendez JA, Lupu R. Fatty acid synthase and the lipogenic phenotype in cancer pathogenesis. *Nat Rev Cancer* 2007;7:763–77. [\[CrossRef\]](#)
7. Flavin R, Peluso S, Nguyen PL, Loda M. Fatty acid synthase as a potential therapeutic target in cancer. *Future Oncol* 2010;6:551–62. [\[CrossRef\]](#)
8. Zhang L, Zhu B, Zeng Y, Shen H, Zhang J, Wang X. Clinical lipidomics in understanding of lung cancer: Opportunity and challenge. *Cancer Lett* 2020;470:75–83. [\[CrossRef\]](#)
9. Li X, Gao S, Li W, Liu Z, Shi Z, Qiu C, et al. Effect of monoacylglycerol lipase on the tumor growth in endometrial cancer. *J Obstet Gynaecol Res* 2019;45:2043–54. [\[CrossRef\]](#)
10. Grabner GF, Zimmermann R, Schicho R, Taschler U. Monoacylglycerol lipase as a drug target: At the crossroads of arachidonic acid metabolism and endocannabinoid signaling. *Pharmacol Ther* 2017;175:35–46. [\[CrossRef\]](#)
11. Zhang H, Guo W, Zhang F, Li R, Zhou Y, Shao F, et al. Monoacylglycerol lipase knockdown inhibits cell proliferation and metastasis in lung adenocarcinoma. *Front Oncol* 2020;10:559568.
12. Zhang J, Song Y, Shi Q, Fu L. Research progress on FASN and MGLL in the regulation of abnormal lipid metabolism and the relationship between tumor invasion and metastasis. *Front Med* 2021;15:649–56.
13. Liu R, Wang X, Curtiss C, Landas S, Rong R, Sheikh MS, et al. Monoacylglycerol lipase gene knockout in mice leads to increased incidence of lung adenocarcinoma. *Cell Death Dis* 2018;9:36.
14. Visweswaran M, Arfuso F, Warriar S, Dharmarajan A. Aberrant lipid metabolism as an emerging therapeutic strategy to target cancer stem cells. *Stem Cells* 2020;38:6–14. [\[CrossRef\]](#)
15. Kienzl M, Hasenoehrl C, Maitz K, Sarsembayeva A, Taschler U, Valadez-Cosmes P, et al. Monoacylglycerol lipase deficiency in the tumor microenvironment slows tumor growth in non-small cell lung cancer. *Oncoimmunology* 2021;10:1965319.
16. Nomura DK, Long JZ, Niessen S, Hoover HS, Ng SW, Cravatt BF. Monoacylglycerol lipase regulates a fatty acid network that promotes cancer pathogenesis. *Cell* 2010;140:49–61. [\[CrossRef\]](#)
17. Wang Y, Zhang H. FAT10 is a Prognostic biomarker and cor-

- related with immune infiltrates in skin cutaneous melanoma. *Front Mol Biosci* 2022;9:805887.
18. Liu X, Xu Q, Li Z, Xiong B. Integrated analysis identifies AQP9 correlates with immune infiltration and acts as a prognosticator in multiple cancers. *Sci Rep* 2020;10:20795. [\[CrossRef\]](#)
 19. Hu L, Zhang P, Sun W, Zhou L, Chu Q, Chen Y. PDPN is a prognostic biomarker and correlated with immune infiltrating in gastric cancer. *Medicine (Baltimore)* 2020;99:e19957. [\[CrossRef\]](#)
 20. Gu Y, Li X, Bi Y, Zheng Y, Wang J, Li X, et al. CCL14 is a prognostic biomarker and correlates with immune infiltrates in hepatocellular carcinoma. *Aging (Albany NY)* 2020;12:784–807.
 21. Xiao Z, Hu L, Yang L, Wang S, Gao Y, Zhu Q, et al. TGF β 2 is a prognostic-related biomarker and correlated with immune infiltrates in gastric cancer. *J Cell Mol Med* 2020;24:7151–62.
 22. Sun H, Jiang L, Luo X, Jin W, He Q, An J, et al. Potential tumor-suppressive role of monoglyceride lipase in human colorectal cancer. *Oncogene* 2013;32:234–41. [\[CrossRef\]](#)
 23. Jiang N, Dai Q, Su X, Fu J, Feng X, Peng J. Role of PI3K/AKT pathway in cancer: the framework of malignant behavior. *Mol Biol Rep* 2020;47:4587–629. [\[CrossRef\]](#)
 24. Zhu W, Zhao Y, Zhou J, Wang X, Pan Q, Zhang N, et al. Monoacylglycerol lipase promotes progression of hepatocellular carcinoma via NF- κ B-mediated epithelial-mesenchymal transition. *J Hematol Oncol* 2016;9:127.
 25. Munson AE, Harris LS, Friedman MA, Dewey WL, Carchman RA. Antineoplastic activity of cannabinoids. *J Natl Cancer Inst* 1975;55:597–602. [\[CrossRef\]](#)
 26. Nithipatikom K, Endsley MP, Isbell MA, Falck JR, Iwamoto Y, Hillard CJ, et al. 2-arachidonoylglycerol: a novel inhibitor of androgen-independent prostate cancer cell invasion. *Cancer Res* 2004;64:8826–30. [\[CrossRef\]](#)
 27. Fowler CJ. Monoacylglycerol lipase - a target for drug development? *Br J Pharmacol* 2012;166:1568–85.
 28. Ma M, Bai J, Ling Y, Chang W, Xie G, Li R, et al. Monoacylglycerol lipase inhibitor JZL184 regulates apoptosis and migration of colorectal cancer cells. *Mol Med Rep* 2016;13:2850–6.
 29. Gong X, Zheng X, Huang Y, Song W, Chen G, Chen T. Monoacylglycerol Lipase (MAGL) inhibition impedes the osteosarcoma progression by regulating epithelial mesenchymal transition. *Tohoku J Exp Med* 2022;256:19–26. [\[CrossRef\]](#)